Continuous Monitoring of Bed-Load Transport in a Laboratory Flume Using an Impact Sensor

Blaise Dhont[1]; Gauthier Rousseau[2]; and Christophe Ancey[3]

Abstract: Bed-load transport rate in gravel-bed rivers shows large non-Gaussian fluctuations, even under steady flow conditions. The development of high-resolution measurement techniques during the last two decades creates research opportunities to study the intermittent character of bed-load transport and the significance of its fluctuations. In this paper, the use of an impact plate as an alternative to video-based technology for laboratory applications is investigated. The objective is to develop a simple and robust technology that can be run continuously over several hours. The impact plate is mounted vertically at the flume outlet. This is a novel nonintrusive configuration, which reduces the uncertainties in the particle transport rate measurement compared with the classical configuration: in that configuration, the impact plate is indeed parallel to the bed and the vibrations recorded by the sensor depend a great deal on the features of particle motion (e.g., the mode of transport, the angle of impact, and the particle velocity). Two key variables were monitored in different flume experiments: the number of moving particles and the bed-load transport rate. They were measured using the vertical plate sensor and image processing. The impact plate and the camera were found to reach the same level of accuracy. The vertical impact plate can therefore be an efficient measurement technique, which requires reduced costs and computational resources. **DOI: 10.1061/(ASCE)HY.1943-7900.0001290.** © *2017 American Society of Civil Engineers.*

Author keywords: Bed-load transport; Indirect measurement; Calibration; Impact plate; Image processing.

Introduction

Prediction models for bed-load transport in gravel-bed rivers are of primary importance to engineering, fluvial geomorphological, and ecological studies (Recking et al. 2008). Most available equations (e.g., Meyer-Peter and Muller 1948; Smart and Jaeggi 1983; Rickenmann 1990; Lefort 1991) have been calibrated from laboratory measurements and are only valid under specific conditions (Turowski and Rickenmann 2011). When applied to mountain rivers, these bed-load transport equations tend to overestimate bed-load transport rates by several orders of magnitude (D'Agostino and Lenzi 1999; Rickenmann 2001; Barry 2004; Comiti and Mao 2012). The development of prediction models therefore continues to attract research efforts (e.g., Ancey 2010; Recking et al. 2012).

Field and laboratory observations have shown that bed-load transport rate exhibits large non-Gaussian fluctuations over time at low water discharges (Ergenzinger 1988), even under steady hydraulic conditions (Gomez and Church 1989; Singh et al. 2009). The intermittent character and the occurrence of large fluctuations of bed-load transport rates are a major challenge for the improvement of bed-load transport equations (Ancey et al. 2014). They arise from several phenomena, including grain sorting (Iseya and Ikeda 1987; Hassan et al. 2006), the destruction and migration of bed forms (Gomez et al. 1989; Recking et al. 2009), limited or varying sediment supply conditions (Benda and Dunne 1997; Recking 2012), and the combined effect of the turbulent nature of the flow and the nonlinear nature of the entrainment and the transport of bed particles (Einstein 1950; Paintal 1971; Ancey et al. 2008).

In order to understand and quantify the effect of these phenomena on bed-load transport rate fluctuations, high-resolution measurements have been identified as a fundamental need for researchers (Marr et al. 2010; Turowski and Rickenmann 2011). As a consequence, the last 20 years have seen great improvements in bed-load transport monitoring technologies that can be operated continuously over long periods of time (i.e., several hours or days). Video-based techniques are gaining popularity in laboratory studies and there is a growing interest for passive acoustic methods applied to field studies. In this paper, the interest is in laboratory techniques.

The classical method for measuring the bed-load transport rate during flume experiments is to collect and weight the sediment at the flume outlet. This technique provides a direct measurement of the bed-load transport rate averaged over the collection period (temporal average) and the cross section (spatial average). It is technically arduous, especially for measurements whose duration is below the minute timescale. For short durations, the experimentalist needs an efficient system to collect and store all sediment samples. Some researchers addressed this drawback by weighing the sediment container at the flume outlet in real time. This approach has two disadvantages: it cannot be operated over extended periods of time because the container must be emptied regularly, and the water jet falling in the container disturbs the measurement.

Image processing has progressed substantially over the last two decades and video-based techniques for measuring bed-load transport rate have developed fast (e.g., Papanicolaou et al. 1999; Keshavarzy and Ball 1999; Frey et al. 2003; Roarty and Bruno 2006; Zimmermann et al. 2008; Bombar et al. 2011). They consist in taking images of a portion of the flume bed at a

[1]Ph.D. Student, Environmental Hydraulics Laboratory, École Polytechnique Fédérale de Lausanne, 1015 Lausanne, Switzerland (corresponding author). E-mail: blaise.dhont@epfl.ch

[2]Ph.D. Student, Environmental Hydraulics Laboratory, École Polytechnique Fédérale de Lausanne, 1015 Lausanne, Switzerland.

[3]Associate Professor, Environmental Hydraulics Laboratory, École Polytechnique Fédérale de Lausanne, 1015 Lausanne, Switzerland.

Note. This manuscript was submitted on July 25, 2016; approved on October 12, 2016; published online on February 7, 2017. Discussion period open until July 7, 2017; separate discussions must be submitted for individual papers. This paper is part of the ***Journal of Hydraulic Engineering***, © ASCE, ISSN 0733-9429.

high frame rate and detecting the moving grains. The major improvements over the traditional method include a continuous monitoring of bed-load transport (subsecond measurement frequency), an extended operational time (up to several hours), and grain size and velocity complementary data. The main limits of the video-based technology are the cost and the need for computational resources to store and process the images.

Passive acoustic methods technologies have raised an increasing interest since the 1990s and have shown promising results for field application. They offer the possibility to provide continuous, nonintrusive, and potentially more accurate bed-load discharge data sets (Gray et al. 2010) over long periods of time (i.e., at least over several days). They may be distinguished in two classes: hydrophones and impact sensors. Hydrophones record the acoustic energy of moving particle impacting other particles (Geay 2013), whereas impact sensors record the energy transmitted by moving grains to an impact structure (e.g., a pipe, a plate, or a column). The sensor fixed on the structure is usually a microphone (Mizuyama et al. 2003, 2010a, b), a geophone (Rickenmann et al. 2014), or an accelerometer (Beylich and Laute 2014). A comprehensive review can be found in Gray et al. (2010). The development of impact sensors is, to the authors' knowledge, devoted to field applications.

This study aims to investigate the use of impact plates as an alternative to video-based technology for bed-load transport monitoring during flume experiments. The motivation is to develop a simple and robust technology that can provide continuous measurements of bed-load transport rate for at least several hours. The impact plate used in this study presents the advantages of being less expensive, easier to operate, and less demanding in terms of computational resources than the camera monitoring system. It was originally developed by Mettra (2014) and Heyman et al. (2013).

The number of moving particles and the bed-load transport rate are measured during several flume experiments. These variables are then used to test the performance of each method. The impact plate is mounted vertically at the flume outlet, a configuration that has, to the best of the authors' knowledge, never been used in the context of sediment transport. Indeed, impact plates have been so far designed for field studies, and the horizontal configuration is the most adapted to this case. Similar systems have been used in other fields such as granular flows (Pecorari 2013). In this experimental study, the vertical configuration is expected to yield better results than impact plates set in flush with the bed. The video-based technique consists of a camera that takes top-view images of the grains moving over a white board placed horizontally at the flume outlet. A particle tracking algorithm is subsequently applied to the images.

Methods

Experimental Setup

Experiments were carried out in a 2.5-m-long and 8-cm-wide tilting flume (Fig. 1). The flume outlet was obstructed by an 11-cm-high metal plate that retained the mobile bed. The upper part of the plate was drilled to drain the bed and avoid resurgence of the subsurface flow near the downstream end of the flume. The water discharge was supplied by a recirculating pump and monitored using an EH Promag (Reinach, Switzerland) 50 flow meter (0.01-L/s uncertainty). Sediment was fed into the flume by a calibrated sediment feeder mounted upstream.

Sediment was collected at the flume outlet over 30-s time intervals (1-s uncertainty) using filtering baskets operated manually. Each sediment sample was dried and weighted (0.01-g uncertainty). The average bed-load transport rate Q_s over 30 s

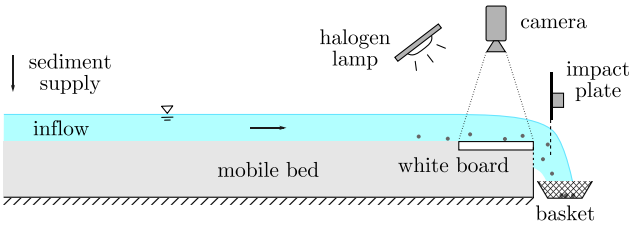

Fig. 1. Schematic of the experimental setup

(3.4% uncertainty) was then computed for each sample. Additionally, top-view images of each sediment sample scattered over a table lit from above were taken. The number of grains N_{part}, the projected area of the grains, and the grain-size distribution were subsequently determined by image processing. The measurements obtained by collecting sediment are the reference against which the impact plate and camera measurements are compared.

Instrumentation

Impact Plate

The impact plate (Fig. 2) consists of an accelerometer and a perforated steel plate (with a hole size of 3 mm), both fixed on an aluminum support plate. The accelerometer is housed in a waterproof aluminum box. The impact plate was mounted vertically 6 cm downstream of the lower end of the flume, in such a way that the grains flushed out from the flume hit the perforated grid only once. The impact plate was insulated from the support frame by a rubber sheet to avoid the transmission of extraneous vibrations.

The accelerometer used in this study was the Three Axis Low-g Micromachined Accelerometer (MMA7361LC) manufactured by Freescale Semiconductor (Austin, Texas). The vibrations due to the grains impacting the plate were monitored by recording the acceleration in the flume direction. Data logging was performed

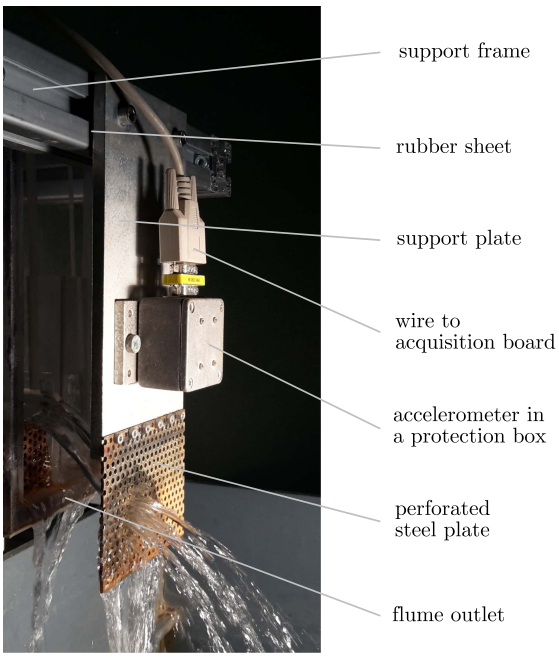

Fig. 2. Impact plate mounted vertically at the flume outlet

in volt using a National Instruments (Austin, Texas) acquisition board with a sampling frequency of 10 kHz.

Camera

A white board (8-cm-wide and 10-cm-long) was mounted horizontally at the flume outlet and illuminated from above by a halogen lamp. A Basler (Ahrensburg, Germany) A504k camera took top-view images of the grains moving over the white board, just before they hit the impact plate. The frame rate was set to 50 frames per second, which was sufficient to capture each grain at least on two images. The camera was placed 72.2 cm above the white board and remotely controlled by a National Instruments acquisition board.

Experimental Procedure

Six experimental runs were conducted. During each experiment, the water discharge, the sediment feed rate, and the flume angle were kept constant. The bed-load transport rate at the flume exit was monitored in parallel by the impact plate, the camera, and the sediment collection. The experimental parameters were changed from one run to another in order to generate various ranges of bed-load transport intensities. The flow conditions were turbulent and supercritical.

Each first three experiments (Runs 1–3) lasted 20 min. The bed material was made of moderately sorted natural gravel of various shapes and colors. The grain-size distribution characteristics were $d_{30} = 5.2$ mm, $d_{50} = 6.0$ mm, $d_{90} = 7.7$ mm, $d_m = 5.5$ mm, and $\sigma_g = 1.2$ mm. The flume angle was set to 8.0% and the water discharge was set to 0.5 L/s.

Each of the last three experiments (Runs 4–6) lasted 10 min. The bed material was made of uniform glass beads, dyed black, with a diameter of 4 mm. The flume width was reduced to 4 mm. Runs 4 and 5 were identical with a water discharge set to 0.2 L/s and a flume angle set to 4.5%. For Run 6, the water discharge was increased to 0.4 L/s and the flume angle was decreased to 3.5%.

Data Processing

Impact Plate

The impact of a single grain on the impact plate generates vibrations that result in oscillations of the accelerometer signal. Therefore, several proxies for bed-load transport can be computed during the signal posttreatement (Rickenmann et al. 2014). In this study, the number of pulses, the number of impulses, and the integral of the signal are considered. An impulse is defined as an oscillation above a threshold amplitude value. An impact generates several impulses, which taken together form a pulse. The proxies are aggregated over 30-s time intervals in order to be compared with the measurements derived from the sediment collection at the flume outlet (N_{part} and Q_s).

The frequencies of the oscillations due to a particle impact typically fall in the 400–700, 1,500–3,000, and 4,000–5,000 Hz ranges. The oscillations are attenuated over a period of approximately 20 ms in the first range of frequencies, and of approximately 10 ms in the last ranges. Therefore, the number of oscillations per single impact is approximately four times greater, and the attenuation period is approximately two times shorter, for the highest frequencies. Additionally, high-pass filters above 1,000 Hz were found the most efficient for background-noise reduction. Hence, only the highest frequencies are considered in the signal posttreatment.

The number of pulses in the signal is indicative of the number of impacts on the impact plate (i.e., the number of particles). The signal posttreatment includes the following steps: (1) background-noise reduction using an eight-order high-pass Butterworth filter at 1,750 Hz; (2) removal of negative values; (3) signal smoothing using a 10-ms moving average (i.e., calculation of the signal envelope); and (4) detection of the peaks greater than 4 mV and wider than 7.5 ms. Each peak is considered as a pulse. The number of pulses detected over 30-s time intervals ($N_{\text{part,acc}}$) is then computed.

The number of impulses was demonstrated to correlate well with the bed-load transport rate (Rickenmann et al. 2014). In this study, it is calculated from the accelerometer signal as follows: (1) background-noise reduction using an eight-order high-pass Butterworth filter at 4,000 Hz; and (2) detection of the impulses that exceed a threshold value of 10 mV. The number of impulses detected over 30-s time intervals (N_{imp}) is then computed, along with the integral of the filtered signal (when it exceeds the threshold value).

Camera

The camera takes 50 top-view images per second of the particles moving over the 8 × 10 cm white board placed at the flume outlet. The images are transformed in real time into binary images and the ratio of black pixels over white pixels is stored. This ratio is subsequently averaged over 30-s time intervals. This variable is named the activity and denoted by A.

If it is assumed that the particle velocity over the white board is constant, the activity A is proportional to the bed-load transport rate. The hypothesis of the constant velocity is justified in this case because the flow over the white board is steady during each run and because the grain-size distribution of the different mixtures used is, at least, relatively narrow.

The raw images taken by the camera are also stored and a particle tracking algorithm is applied during postprocessing. The number of moving particles detected over 30-s time intervals ($N_{\text{part,cam}}$) is computed, along with the average projected area and the mean velocity of each particle.

Results

The impact plate and the camera measurements for the number of particles and the bed-load transport rate are presented in this section. The measurements derived from the sediment collection at the flume outlet (N_{part} and Q_s) are used as a reference to assess the precision of the impact plate and the camera methods.

Number of Particles

The number of particles flushed out from the canal over 30-s intervals (N_{part}) was measured with the impact plate ($N_{\text{part,acc}}$) and the camera ($N_{\text{part,cam}}$). The results are presented in Fig. 3. The experiments with glass beads (Runs 4–6) and with natural gravel (Runs 1–3) are different because measurements in the latter can be affected by variation in grain size and shape. Both methods are direct measurements but may require calibration. The regression curves between the measured and the actual values of the variable are therefore computed and compared against the $y = x$ curve. The coefficients of determination (R^2) and the standard errors (SEs) are summarized in Table. 1.

Calibration and Measuring Precision

Regression analysis for the glass bead experiments shows a linear relationship between $N_{\text{part,cam}}$ and N_{part}, and between $N_{\text{part,acc}}$ and N_{part} [Figs. 3(b and d)]. The measuring precision is comparable for the two methods (standards errors < 5 grains/30 s). However, the impact plate underestimates the number of particles and requires calibration, whereas the regression curve for the camera matches the $y = x$ curve.

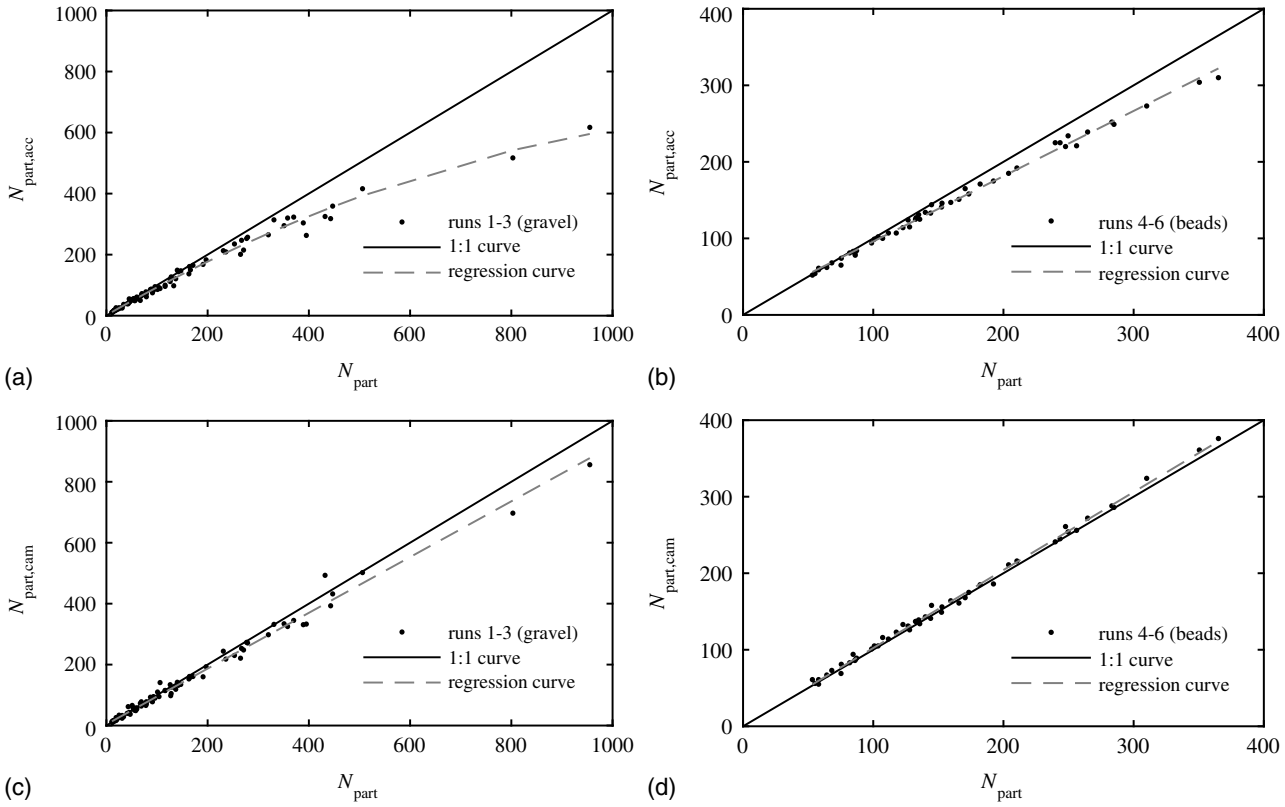

Fig. 3. Relationship between the number of grains flushed out from the canal and (a) the number of grains measured by the accelerometer for natural gravel; (b) the number of grains measured by the accelerometer for glass beads; (c) the number of grains measured by the camera for natural gravel; (c) the number of grains measured by the camera for glass beads; the solid lines are the 1:1 curves representing the perfect fit and the dashed lines are the regression curves (equations are given in Table 1)

Table 1. Summary of the Regression Analysis between the Number of Grains Measured by the Accelerometer and the Camera and the Actual Number of Grains

Variable	Run	N_s[a]	R^2	SE[b]	Regression curve
$N_{part,cam}$	1–3 (gravel)	120	0.99	13.98	$y = 0.91x + 3.91$
$N_{part,cam}$	4–6 (beads)	50	1.00	4.63	$y = 1.02x + 0.36$
$N_{part,acc}$	1–3 (gravel)	120	0.97	20.02	$y = 0.73x + 13.16$
$N_{part,acc}$	1–3 (gravel)	120	0.99	11.38	$y = -0.0003x^2 + 0.95x + 1.67$
$N_{part,acc}$	4–6 (beads)	50	0.99	4.80	$y = 0.85x + 10.72$
$N_{part,acc}$	4–6 (beads)	50	1.00	3.93	$y = -0.0004x^2 + 1.00x - 0.60$

[a]Number of samples.
[b]Standard error in grains per 30 s.

For the natural gravel experiments, the range of N_{part} values is wider. The calibration curve is quadratic for the impact plate and linear for the camera [Figs. 3(a and c)]. The measuring precision is slightly higher for the first method (the standard errors are respectively 11.4 and 14.0 grains/30 s).

The measuring precision is lower for natural gravel than for glass beads. This was expected because beads uniform in size, shape, and color are easier to detect than natural grains (for both methods). The slight underestimation of the camera measurements is due to the small grains and light-color grains that can be missed. The quadratic calibration curve of the impact plate indicates that the sensor saturates for high bed-load transport rates (>60 grains/30 s).

Saturation of the Impact Plate

The saturation of the impact plate is likely due to the arrival of grain clusters. Indeed, when several grains hit the sensor over a very short time, it can be difficult to distinguish the different impacts in the accelerometer signal. This hypothesis is tested comparing the cluster rates with the errors of prediction $N_{part,acc} - N_{part}$.

The cluster rate in each 30-s sample is defined as the proportion of grains whose interarrival time is less than 60 ms. This threshold value was chosen so that the correlation with the errors of prediction is maximized. It is of the same order of magnitude as the duration of an impact, which is physically significant.

The cluster rates are computed based on the camera measurements, which accurately estimate the number of particles. Only the samples for which $N_{part,cam} = N_{part} \pm 10\%$ are taken into account for consistency (48 samples for the glass bead experiments and 63 samples for the natural gravel experiments).

The errors of prediction are compared with the cluster rates for the glass bead experiments (Fig. 4). They cannot be affected by variation in grain size and shape in this case. The positive residuals are not taken into account (46 remaining samples). The result indicates a strong negative correlation that can be described by a power law ($R^2 = 0.87$ and standard error = 4.7 grains).

This observation indicates that grain clusters are the main cause for the saturation of the impact plate. Additionally, the cluster rate is found to be linearly correlated with the number of particles (correlation coefficient $r = 0.95$). This was expected because the probability of observing short interarrival times increases with the number of particles.

Correction for Grain Clusters

In order to take into account the saturation effect due to grain clusters, $N_{part,acc}$ is corrected for each sample using the power law derived for glass beads ($y = -227.7x^{2.5}$) and the cluster rate as follows:

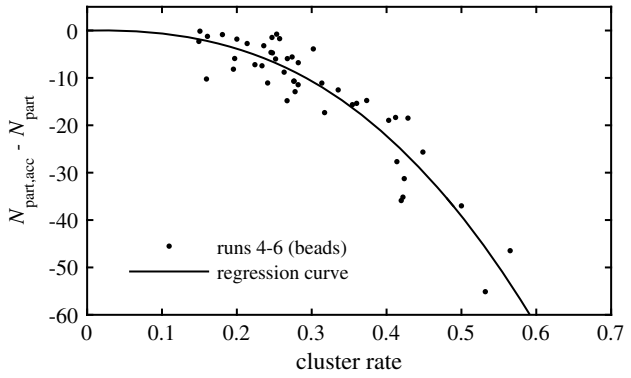

Fig. 4. Relationship between the errors of prediction $N_{part,acc} - N_{part}$ and the cluster rates for glass beads; the solid line is the power regression curve $y = -227.7x^{2.5}$

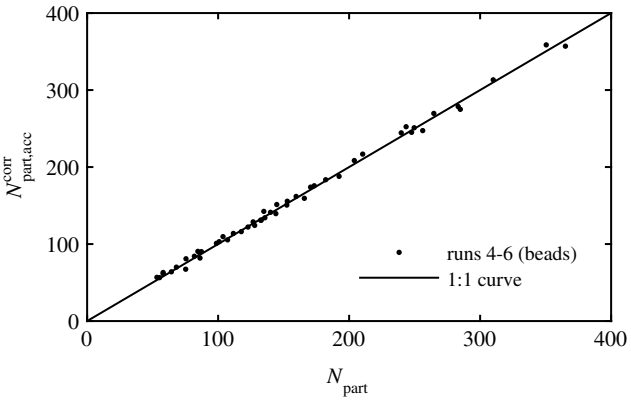

Fig. 5. Relationship between the corrected number of grains measured by the accelerometer and the actual number of grains flushed out from the canal for glass beads; the solid line is the 1:1 curve representing the perfect fit

$$N^{corr}_{part,acc} = N_{part,acc} + 227.7(\text{cluster rate})^{2.5}$$

For glass beads, the relation between $N^{corr}_{part,acc}$ and N_{part} is linear ($R^2 = 1.00$) and matches the $y = x$ curve (Fig. 5). The standard errors of the calibration curves for $N^{corr}_{part,acc}$ (linear) and $N_{part,acc}$ (quadratic) are comparable (respectively, 4.7 and 3.9 grains/30 s).

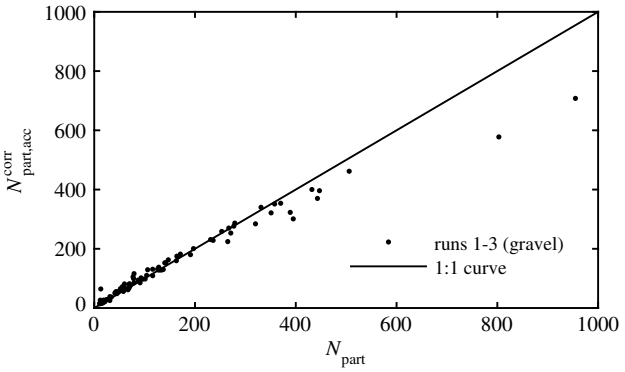

Fig. 7. Relationship between the corrected number of grains measured by the accelerometer and the actual number of grains flushed out from the canal for natural gravel; the solid line is the 1:1 curve representing the perfect fit

The same correction is applied to the impact plate measurements for the natural gravel experiments. However, because there is likely a minimum size for detection, the cluster rates have to be computed by ignoring the smallest fraction of the grains.

The projected area of the grains is used here as a proxy for grain size because it can be directly calculated from the camera measurements. The errors of prediction $N_{part,acc} - N_{part}$ are compared with the adjusted cluster rates for several grain-size threshold values. The relationship is found similar to the one for glass beads when grains smaller than 25 mm^2 are ignored [Fig. 6(b)].

The $N_{part,acc}$ for natural gravel is then corrected by using the adjusted cluster rates and the power law derived for glass beads (Fig. 7). The relationship with N_{part} matches the $y = x$ curve ($R^2 = 0.92$ and standard error = 36.5 grains). This supports the conclusion that grain clusters cause saturation of the impact plate. Furthermore, it enlightens the fact that the fine fraction of the natural gravel is not (or partially) detected by the accelerometer.

Minimum Grain Size for Detection

In order to evaluate the minimum grain size detected by the impact plate, the number of grains measured in each sample (N_{part}) is corrected ($N_{part,corr}$) by ignoring the smallest fraction. The projected area of the grains is used as a proxy for grain size (see previous section). The quadratic calibration curve for $N_{part,acc}$ and $N_{part,corr}$ is then computed for different area threshold values. The relationship between the standard error and the area threshold value is presented in Fig. 8.

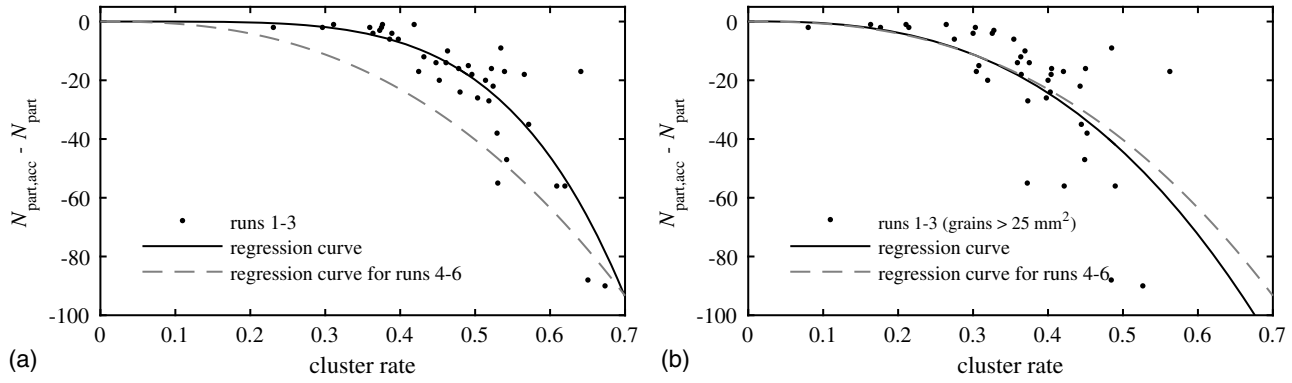

Fig. 6. Relationship between the errors of prediction $N_{part,acc} - N_{part}$ and the cluster rates for natural gravel (a) considering all grains and (b) considering only the grains larger than 25 mm^2; the solid lines are the power regression curves $y = -484.4.8x^{4.6}$ in (a) and $y = -287.3x^{2.7}$ in (b) for natural gravel; the dashed line is the power regression curve $y = -227.7x^{2.5}$ for glass beads

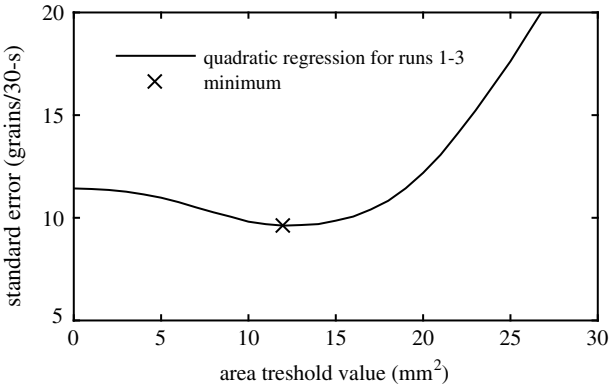

Fig. 8. Standard error of the quadratic regression between $N_{\text{part,acc}}$ and $N_{\text{part,corr}}$ as a function of the threshold area value used to compute $N_{\text{part,corr}}$

It indicates that the standard error is minimized for an area threshold value of 12 mm^2, which corresponds to an average diameter of 4 mm. This value can therefore be interpreted as the minimum grain size for detection for the natural gravel mixture. It is consistent with the value estimated in the previous section (25 mm^2).

The beads are detected by the impact plate although they are 4 mm in diameter. This is because the gravel grains are flat. Their mass is therefore less than the one of spherical beads of the same average diameter (the size is used as a proxy for the mass, which is the limiting factor for detection). No minimum grain size for detection by the camera could be computed with the gravel mixture used in this study.

Bed-Load Transport Rate

The bed-load transport rate at the flume outlet is measured indirectly by the camera and the impact plate. The proxies are respectively the activity A and the number of impulses N_{imp}. In this section, they are compared with the reference values of the bed-load transport rate Q_s. All variables are averaged over 30-s time intervals for comparison.

Calibration and Measuring Precision

For the glass bead experiments, the relationships between A and Q_s, and between N_{imp} and Q_s, are both linear (Fig. 9). The measuring precision is higher for the camera than for the impact plate (standard errors are, respectively, 20 and 60 mg/s, and R^2 coefficients are, respectively, 0.99 and 0.94). However, when only one experiment is considered, the precisions of the two measurement methods are comparable. This is because the regression curve of the impact plate varies from one experiment to another.

It indicates a dependence of the calibration curve on the water discharge and/or the flume angle because they are the only parameters that changed. For instance, one can expect the pressure of the water jet on the metallic plate to modify the vibratory response of the device.

For the natural gravel experiments, the camera settings were changed from one experiment to another to adjust for the ambient luminosity. As a consequence, the calibration curves differ. Experiment 3, which recorded the widest range of bed-load discharge values, is chosen for the comparison of the two measurement methods (Fig. 10). The N_{imp} and A are both linearly correlated with Q_s ($R^2 > 0.98$), but the impact plate is more precise (standard error = 0.16 g/s) than the camera (standard error = 0.24 g/s). No saturation effect is observed within the range of values studied.

Effect of Grain Size and Velocity

The relationship between the particle size and the accelerometer response is first studied using the data derived from the sediment collected at the flume outlet. For each 30-s sample of the natural gravel experiments, the number of grains and the average grain size are computed. The average grain size is then compared with the average number of impulses per grain [Fig. 11(a)] and with the integral of the signal divided by the number of grains. The correlation coefficients r are, respectively, 0.67 and 0.74. This indicates that when coarser grains impact the sensor, the number of oscillations in the signal is higher and their amplitudes tend to be larger.

The effect of particle size and velocity on the accelerometer response is further studied by matching the camera measurements with the accelerometer measurements. Particle size and velocity data are thus available for a number of impacts in the accelerometer signal. The number of impulses, the integral of the filtered signal when it exceeds the threshold value of 10 mV, and the maximum amplitude of the filtered signal are computed for each impact.

The particle velocity distribution for the glass bead experiments is normal and defined by a mean value of 0.4 m/s and a standard deviation of 0.04 m/s. Within this range of values, the number of impulses per impact is not correlated with the particle velocity. There is no particle-size effect for the glass bead experiments. For the natural gravel experiments, the range of particle velocity values is wider (mean = 0.5 m/s and standard deviation = 0.09 m/s). The particle velocity and the number of impulses per impact are also

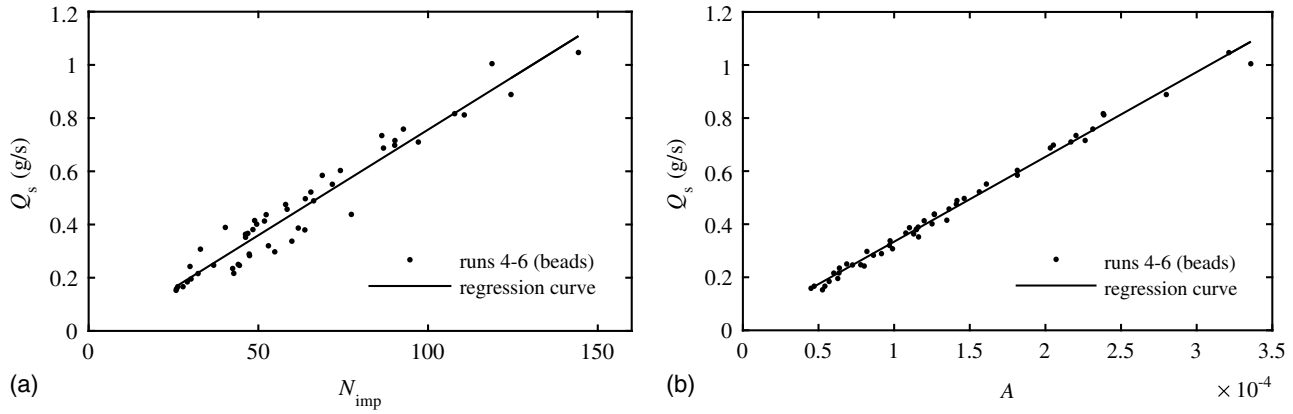

Fig. 9. Relationship between the bed-load transport rate Q_s and (a) the number of impulses N_{imp}; (b) the activity A, for glass beads; the solid lines are the linear regression curves

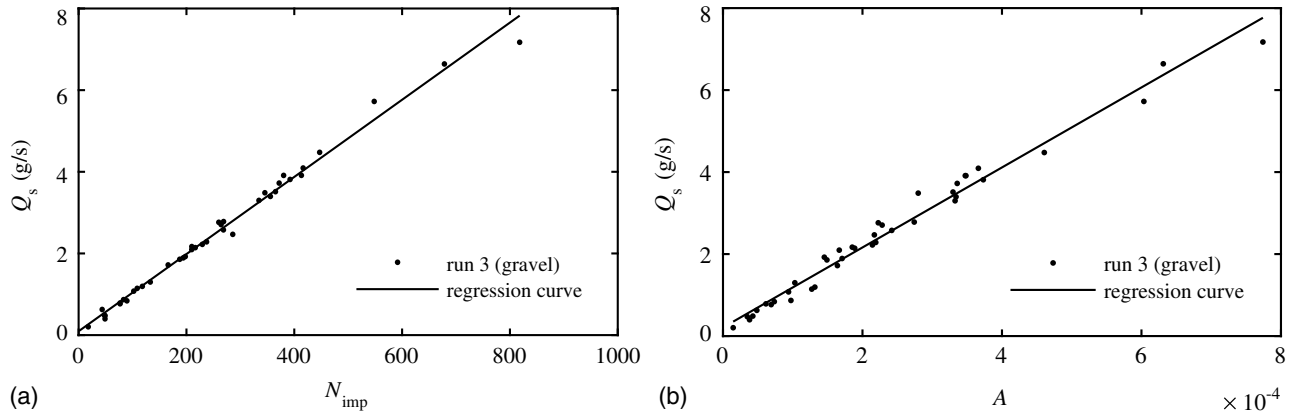

Fig. 10. Relationship between the bed-load transport rate Q_s and (a) the number of impulses N_{imp}; (b) the activity A, for Run 3 (natural gravel); the solid lines are the linear regression curves

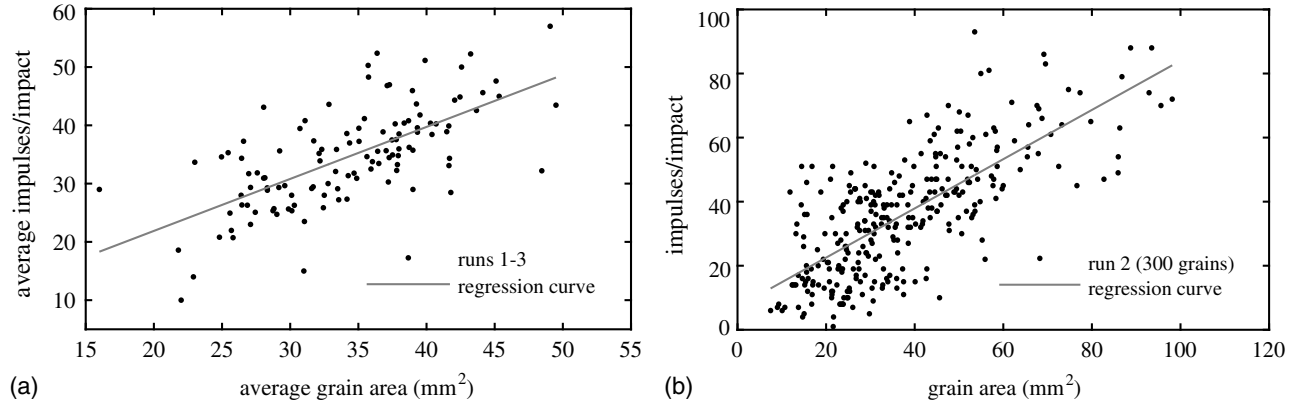

Fig. 11. (a) Relationship between the average number of impulses per impact and the average particle projected area for the 120 samples from Runs 1–3; (b) relationship between the number of impulses per impact and the particle projected area for 300 grains from Run 2; the solid lines are the linear regression curves

found to be independent. Additionally, the particle velocity neither correlates with the integral of the signal nor the maximum amplitude for any of the experiments.

The effect of particle size on the accelerometer response is studied for the natural gravel experiments. The matching of the accelerometer and the camera measurements yields good results for Run 2 (300 matches). The result [Fig. 11(b)] indicates that the particle size is positively correlated with the number of impulses per impact (correlation coefficient $r = 0.76$). The correlation with the integral of the signal and the maximum amplitude shows a positive tendency, but the relation is too noisy to draw any conclusion.

Discussion

Comparison of the Two Measurement Techniques

In this section, the results from the impact plate and the camera are compared for the two variables of interest: the number of particles and the bed-load transport rate. The comparison is performed based on the results obtained for the experiments with natural gravel. Indeed, the latter are more representative of usual experimental conditions when studying bed-load transport in a gravel-bed flume. The advantages and disadvantages of each technique are then discussed.

Number of Particles

The bed-load transport rate is often defined as the number of particles moving across a given cross section, or in a given control volume, over a certain period of time (e.g., Ancey et al. 2008). It is then usually measured using video-based techniques (e.g., Heyman et al. 2014). This study shows that the impact plate and the camera measurements have the same standard error, which is less than 3 grains/30 s when the bed-load transport rate is below 30 grains/30 s. The results are compared over 30-s time intervals for consistency (see previous section).

The impact plate sensor was found to saturate because of the arrival of grain clusters for high bed-load transport rates (>2 grains/s). It is recalled that the 90th percentile of the number of particles recorded per 30-s sample was 325 grains/30 s (the maximum was 955 grains/30 s). This saturation effect can be taken into account using a quadratic calibration curve instead of a linear calibration curve. The measuring precision of the impact plate is then comparable to the one of the camera and both standard errors are below 14 grains/30 s.

For rates below 1 grains/s, both techniques performed very well. Beylich and Laute (2014) observed the same result when testing an impact plate in a flume. However, they indicated that for higher rates their device could only detect the start and end of bed-load transport. This study show that good results can be

obtained by the impact plate for higher rates (up to 10 grains/s), although saturation of the sensor occurs.

In this study, the level of saturation (i.e., the cluster rate) is modeled as a function of the number of moving particles during a given time interval (30 s in these experiments), which is an approximation. The cluster rate depends on the interarrival time of the moving particles during the time interval. Therefore, the camera technique is believed to be a more robust method to measure the number of grains, especially for grain transport rates above 1 grain/s. A saturation effect is also likely to occur for the camera (e.g., if moving grains overlap), but for much higher rates than the impact plate.

Bed-Load Transport Rate

The bed-load transport rate is commonly expressed as an average mass (or volume) of sediment transported per unit time over a certain period of time. In this study, the bed-load transport rates are averaged over 30-s time intervals, which is the sediment weighing frequency. It is recalled that the number of impulses (impact plate) and the activity (camera) are the chosen proxies for the bed-load transport rate.

The impact plate measurements are more precise than the camera measurements. The third experiment, with natural gravel, is chosen as an example for comparison. The bed-load transport rates recorded range from 0 to 7.17 g/s, or from 0 to 89 $gs^{-1}\,m^{-1}$ if expressed per unit width. Given the average mass of the gravel grains (0.23 g), this range is considered relatively large for a flume experiment.

Within this range of bed-load transport rate values, the relative standard errors of measurement vary little. They are between 2.3 and 2.6% for the impact plate and 3.5 and 3.8% for the camera. Therefore, the impact plate performs better than the camera, even for relatively high bed-load transport rates. The lowest accuracy of the camera can be partially due to the variability in the particle velocity at the flume outlet. Indeed, the bed-load transport rate is a function of the product of the activity and the particle velocity.

The impact plate does not saturate when measuring the bed-load transport rate, whereas it does when measuring the number of particles. This indicates that the number of impulses is a robust proxy of the bed-load transport rate, as reported by Rickenmann et al. (2014). For even higher rates, both measurement techniques are expected to saturate and neither would be appropriate. The accuracies of the impact plate measurements are difficult to compare with the literature because most authors used impact plate under field conditions and only reported the coefficients of determination of the calibration curves (which depend on the number of samples).

Further Considerations

The impact plate and the camera yield measurements of comparable precision and demand similar efforts for implementation. Other considerations are therefore discussed.

The impact plate has the advantage of being more cost-effective and of demanding less computational resources than the camera. Indeed, the latter requires a camera device, which can be expensive, and the image storage and processing cost digital memory and computation time. The need for computational resources can be reduced by computing the activity (i.e., the proxy for bed-load transport) for each image in real time. However, applying a particle-tracking algorithm to the raw images during postprocessing can provide grain size and velocity data, which can be of interest.

The major advantage of the impact plate compared with the camera is the minor dependence of the calibration curve on the device settings (once the device is mounted). Indeed, the calibration curve of the camera depends on the camera settings (e.g., the aperture, the shutter speed, and the image resolution) and on the ambient luminosity. The latter can be particularly difficult to control.

The calibration curve of the impact plate depends on experimental settings such as the grain size and, to a lesser extent, the liquid discharge. It implies that the calibration curve has to be verified, and adjusted if necessary, when these parameters are changed. For the camera, only the water height at the flume outlet can potentially affect the calibration curve.

The impact plate cannot detect grains smaller than a certain size. In this study, it is estimated to approximately 4 mm in average diameter. No minimum size could be computed for the camera with the gravel mixture used. It was observed that light-color grains can be missed by the video-based technique. Moreover, the bed-load transport rate measured by the camera depends on the grain shapes because it is based on the projected areas.

The impact plate is more likely to saturate than the camera. Indeed, in the first case the sensor saturates when the interarrival of the grain is very short. In the second case, it occurs when the grains overlap, which is rarer.

As a conclusion, when to use of one or the other method depends on the experimental setup. The use of the impact plate is suggested for the long-term monitoring (e.g., several hours) of bed-load transport rates, under the condition that the bed material is sufficiently coarse and the range of liquid discharges is relatively narrow. The camera is more appropriate when the experiments are of shorter duration and when grain size and velocity data are needed.

Impact Plate

Several researchers used impact plates to monitor bed-load transport. However, these studies were, to the authors' knowledge, motivated by field applications, whereas the impact plate presented here is essentially devoted to laboratory experiments.

This results in two major differences. First, impact plates conceived for field experiments are set flush with the bed (horizontal configuration). In this study, the impact plate was mounted vertically at the flume outlet. The latter configuration is not adapted to field conditions. Indeed, its use is limited to a restricted range of water discharges and grain sizes. Moreover, it requires a weir, which generates additional costs.

Second, impact plates for field application are designed to resist great mechanical stresses and to monitor the movement of coarse grains (e.g., >10 mm in diameter). The bed material used in flume experiments is generally finer than the material found in natural gravel-bed rivers (because of the geometric similarity). As a consequence, the device used here was designed to monitor the transport of relatively fine gravel (<10 mm in diameter).

Given the preceding considerations, it is necessary to be careful when comparing the impact plate presented here with other devices developed for field applications.

The response of the accelerometer signal to the impact of particles in this study is similar to the response of the output signal of field impact plates. The signal postprocessing algorithms are therefore comparable. As in other studies, the number of particles is herein directly obtained by counting the number of pulses (i.e., impacts) in the signal.

Postprocessing for bed-load transport rates is less straightforward. For instance, Rickenmann et al. (2014) proposed several proxies for bed-load transport rates: the number of impulses over a threshold amplitude, the integral of the signal, and the quadratic integral of the signal. The primer was found the most robust proxy. This study supports this result: the number of impulses was found to be linearly correlated with the bed-load transport rate.

The use of horizontal impact plates is not limited to field conditions. They have been successfully used in laboratory flumes (Beylich and Laute 2014; Tsakiris et al. 2014; Barrière et al. 2015), usually for tests before implementation in the field. The main advantage of the horizontal configuration is that the device can be placed along any cross section of the flume, whereas the device in a vertical configuration can be only mounted at the lower end of the flume. However, the vertical configuration is nonintrusive, while the horizontal one locally modifies the bed. Moreover, the vertical configuration has several important advantages detailed subsequently. Indeed, this configuration reduces the variability in the signal response to the impact of a same particle.

Beylich and Laute (2014) observed in their experiment that moving particles could impact the impact plate more than one time, which obviously leads to an overestimation of the measurement. Conversely, measurement underestimation arises from particles jumping over the impact plate. These effects are almost absent for a vertical configuration of the impact plate.

Rickenmann et al. (2014) and Tsakiris et al. (2014) reported that the particle transport mode (e.g., rolling or saltating) can affect the response of the impact plate. In the vertical configuration, all the particles hit the impact plate in the same manner. The variability in the signal response due to the transport mode is eliminated.

The impact plate response depends on the particle velocity at the moment of impact (Beylich and Laute 2014; Rickenmann et al. 2014). In the vertical configuration, this source of variability is reduced compared with the horizontal configuration. Indeed, because the particle velocity highly depends on the flow velocity, the particle velocity distribution of the particles flushed out from the flume is believed to be narrower than the one of the particles hitting a horizontal impact plate placed somewhere along the bed. No effect of particle velocity was observed in this study.

A central question concerning the calibration of impact plates is the effect of grain size on the signal response. This study shows, as pointed by other researchers (e.g., Rickenmann et al. 2014), that the size of the hitting particle is positively correlated with the number of impulses per impact. As a consequence, the precision of the measurement is expected to decrease with increasing width of the grain-size distribution. For a given grain-size distribution, this effect is accounted for in the confidence interval of the calibration curve.

The impact plate presented here was tested with a narrow particle-size distribution. Arguably, results should remain satisfactory for wider size distributions. Wyss et al. (2016) have indeed shown that the signature of each grain class can be detected in vibration signals, and it is expected that similar treatment could be done with the vertical plate.

Conclusion

The results of this study have shown that the impact plate and the camera perform well at measuring the bed-load transport rate and the number of particles under laboratory conditions as long as the bed-load transport intensity is not too high. The signal recorded by the impact plate saturates as soon as particles do not impact the plate individually, but collectively in the form of clusters. Because the grain clustering rate is related to the number of particles, this saturation effect can be corrected using a quadratic equation instead of a linear equation for the calibration curve.

The impact plate presented in this study is mounted vertically instead of horizontally, as is the case in other studies. Its use is therefore limited to laboratory conditions and to measurements at the flume outlet. Several advantages arise from this new configuration: it is nonintrusive, particles hit the sensor only once, there is no effect of the particle mode of transport on the accelerometer signal, and the variability in the particle velocities and the particle trajectories at the moment of impact is reduced. In agreement with other studies, the number of impulses in the accelerometer signal was found to be a robust proxy for the bed-load transport rate, and a positive effect of the grain size on the accelerometer signal was observed.

The disadvantages of the camera compared with the impact plate include the price, the need for extended computational resources, the dependence of the calibration curve on the device settings (e.g., ambient luminosity), and the restriction to dark-color grains. Moreover, when using the activity as the proxy for the bed-load transport rate, the calibration curve depends on the grain velocity.

The drawbacks of the impact plate include the dependence of the calibration curve on the experimental settings (e.g., grain size and velocity), the possible saturation of the sensor for high bed-load transport rates, and the minimum grain size for detection. Moreover, the camera can provide complementary data about grain size and velocity when a particle-tracking algorithm is applied to images (which requires computational resources).

As a conclusion, the impact plate can be used as an alternative to video-based techniques when the experimental setup is compatible with vertical plates. The impact plate is recommended for the continuous monitoring of bed-load transport rates over long periods of time (up to several days). The camera technique is better suited to short experiments when particle size and velocity are of interest.

Acknowledgments

The authors acknowledge the support of the Swiss National Science Foundation (Grant 200021_129538 for a project called "The Stochastic Torrent: Stochastic Model for Bed Load Transport on Steep Slope"). They also thank the editorial board and two anonymous reviewers for the constructive comments that helped improve the initial manuscript.

References

Ancey, C. (2010). "Stochastic modeling in sediment dynamics: Exner equation for planar bed incipient bed load transport conditions." *J. Geophys. Res.: Earth Surf.*, 115(F2), F00A11.

Ancey, C., Bohorquez, P., and Bardou, E. (2014). "Sediment transport in mountain rivers." *ERCOFTAC Bulletin*, 100, 37–52.

Ancey, C., Davison, A. C., Boehm, T., Jodeau, M., and Frey, P. (2008). "Entrainment and motion of coarse particles in a shallow water stream down a steep slope." *J. Fluid Mech.*, 595, 83–114.

Barrière, J., Krein, A., Oth, A., and Schenkluhn, R. (2015). "An advanced signal processing technique for deriving grain size information of bedload transport from impact plate vibration measurements." *Earth Surf. Processes Landforms*, 40(7), 913–924.

Barry, J. J. (2004). "A general power equation for predicting bed load transport rates in gravel bed rivers." *Water Resour. Res.*, 40(10), W10401.

Benda, L., and Dunne, T. (1997). "Stochastic forcing of sediment supply to channel networks from landsliding and debris flow." *Water Resour. Res.*, 33(12), 2849–2863.

Beylich, A. A., and Laute, K. (2014). "Combining impact sensor field and laboratory flume measurements with other techniques for studying fluvial bedload transport in steep mountain streams." *Geomorphology*, 218, 72–87.

Bombar, G., Elci, S., Tayfur, G., Guney, S., and Bor, A. (2011). "Experimental and numerical investigation of bed-load transport under

unsteady flows." *J. Hydraul. Eng.*, 10.1061/(ASCE)HY.1943-7900.0000412, 1276–1282.
Comiti, F., and Mao, L. (2012). *Gravel-bed rivers: Processes, tools, environments*, Wiley, Chichester, U.K., 351–377.
D'Agostino, V., and Lenzi, M. A. (1999). "Bedload transport in the instrumented catchment of the Rio Cordon. Part II: Analysis of the bedload rate." *CATENA*, 36(3), 191–204.
Einstein, H. A. (1950). "*The bed-load function for sediment transportation in open channel flows*." *Technical Bulletin No. 1026*, U.S. Dept. of Agriculture, Washington, DC.
Ergenzinger, P (1988). "The nature of coarse material bed load transport." *Sediment Budgets: Proc., Symp. Held at Porto Alegre*, M. P. Bordas and D. E. Walling, eds., Vol. 174, IAHS Press, Wallingford, U.K., 207–216.
Frey, P., Ducottet, C., and Jay, J. (2003). "Fluctuations of bed load solid discharge and grain size distribution on steep slopes with image analysis." *Exp. Fluids*, 35(6), 589–597.
Geay, T. (2013). "Mesure acoustique passive du transport par charriage dans les rivières." Ph.D. thesis, Université de Grenoble, Grenoble, France.
Gomez, B., and Church, M. (1989). "An assessment of bed load sediment transport formulae for gravel bed rivers." *Water Resour. Res.*, 25(6), 1161–1186.
Gomez, B., Naff, R. L., and Hubbell, D. W. (1989). "Temporal variations in bedload transport rates associated with the migration of bedforms." *Earth Surf. Processes Landforms*, 14(2), 135–156.
Gray, J. R., Laronne, J. B., and Marr, J. D. (2010). "Bedload-surrogate monitoring technologies." *Rep. 2010-5091*, U.S. Geological Survey Scientific Investigations, Reston, VA.
Hassan, M. A., Egozi, R., and Parker, G. (2006). "Experiments on the effect of hydrograph characteristics on vertical grain sorting in gravel bed rivers." *Water Resour. Res.*, 42(9), W09408.
Heyman, J., Ma, H. B., Mettra, F., and Ancey, C. (2014). "Spatial correlations in bed load transport: Evidence, importance, and modeling." *J. Geophys. Res.: Earth Surf.*, 119(8), 1751–1767.
Heyman, J., Mettra, F., Ma, H. B., and Ancey, C. (2013). "Statistics of bedload transport over steep slopes: Separation of time scales and collective motion." *Geophys. Res. Lett.*, 40(1), 128–133.
Iseya, F., and Ikeda, H. (1987). "Pulsations in bedload transport rates induced by a longitudinal sediment sorting: A flume study using sand and gravel mixtures." *Geografiska Annaler. Ser. A, Phys. Geogr.*, 69(1), 15–27.
Keshavarzy, A., and Ball, J. (1999). "An application of image processing in the study of sediment motion." *J. Hydraul. Res.*, 37(4), 559–576.
Lefort, P. (1991). *Transport solide dans le lit des cours d'eau—Dynamique fluviale (lecture notes)*, Ecole Nationale Supérieure d'Hydraulique et de Mécanique de Grenoble, Grenoble, France.
Marr, J. D., Gray, J. R., Davis, B. E., Ellis, C., and Johnson, S. (2010). "Large-scale laboratory testing of bedload-monitoring technologies; overview of the StreamLab06 experiments." *Rep. 2010-5091*, Bedload-surrogate monitoring technologies, U.S. Geological Survey Scientific Investigations, Reston, VA, 266–282.
Mettra, F. (2014). "Morphodynamic mechanisms in steep channels: From local processes to large-scale evolution." Ph.D. thesis, École Polytechnique Fédérale de Lausanne, Lausanne, Switzerland.
Meyer-Peter, E., and Muller, R. (1948). *Formulas for bed-load transport*, International Association for Hydraulic Research, Stokholm, Sweden, 39–64.
Mizuyama, T., et al. (2010a). "Calibration of a passive acoustic bedload monitoring system in Japanese mountain rivers." *Rep. 2010-5091*, U.S. Geological Survey Scientific Investigations, Reston, VA.
Mizuyama, T., Fujita, M., and Nonaka, M. (2003). "Measurement of bed load with the use of hydrophones in mountain torrents." *Erosion and sediment transport measurement in rivers: Technological and methodological advances*, IAHS Press, Wallingford, U.K., 222–227.
Mizuyama, T., Oda, A., Laronne, J. B., Nonaka, M., and Matsuoka, M. (2010b). "Laboratory tests of a Japanese pipe geophone for continuous acoustic monitoring of coarse bedload." *Rep. 2010-5091*, U.S. Geological Survey Scientific Investigations, Reston, VA.
Paintal, A. S. (1971). "A stochastic model of bed load transport." *J. Hydraul. Res.*, 9(4), 527–554.
Papanicolaou, A. N., Diplas, P., Balakrishnan, M., and Dancey, C. L. (1999). "Computer vision technique for tracking bed load movement." *J. Comput. Civ. Eng.*, 10.1061/(ASCE)0887-3801(1999)13:2(71), 71–79.
Pecorari, C. (2013). "Characterizing particle flow by acoustic emission." *J. Nondestr. Eval.*, 32(1), 104–111.
Recking, A. (2012). "Influence of sediment supply on mountain streams bedload transport." *Geomorphology*, 37(7), 774–789.
Recking, A., Frey, P., Paquier, A., and Belleudy, P. (2009). "An experimental investigation of mechanisms involved in bed load sheet production and migration." *J. Geophys. Res.: Earth Surf.*, 114(F3), F03010.
Recking, A., Frey, P., Paquier, A., Belleudy, P., and Champagne, J. Y. (2008). "Feedback between bed load transport and flow resistance in gravel and cobble bed rivers." *Water Resour. Res.*, 44(5), W05412.
Recking, A., Liébault, F., Peteuil, C., and Jolimet, T. (2012). "Testing bedload transport equations with consideration of time scales." *Earth Surf. Processes Landforms*, 37(7), 774–789.
Rickenmann, D. (1990). "Bedload transport capacity of slurry flows at steep slopes." Ph.D. thesis, ETH Zürich, Zürich, Switzerland.
Rickenmann, D. (2001). "Comparison of bed load transport in torrents and gravel bed streams." *Water Resour. Res.*, 37(12), 3295–3305.
Rickenmann, D., et al. (2014). "Bedload transport measurements with impact plate geophones: Comparison of sensor calibration in different gravel-bed streams." *Earth Surf. Processes Landforms*, 39(7), 928–942.
Roarty, H. J., and Bruno, M. S. (2006). "Laboratory measurements of bed load sediment transport dynamics." *J. Waterway, Port, Coastal, Ocean Eng.*, 10.1061/(ASCE)0733-950X(2006)132:3(199), 199–211.
Singh, A., Fienberg, K., Jerolmack, D. J., Marr, J., and Foufoula-Georgiou, E. (2009). "Experimental evidence for statistical scaling and intermittency in sediment transport rates." *J. Geophys. Res.: Earth Surf.*, 114(F1), F01025.
Smart, G. M., and Jaeggi, M. (1983). "Sediment transport on steep slopes." Technical Rep.ETH Zürich, Zürich, Switzerland.
Tsakiris, A. G., Papanicolaou, A. T. N., and Lauth, T. J. (2014). "Signature of bedload particle transport mode in the acoustic signal of a geophone." *J. Hydraul. Res.*, 52(2), 185–204.
Turowski, J. M., and Rickenmann, D. (2011). "Measuring the statistics of bed-load transport using indirect sensors." *J. Hydraul. Eng.*, 10.1061/(ASCE)HY.1943-7900.0000277, 116–121.
Wyss, C. R., Rickenmann, D., Fritschi, B., Turowski, J. M., Weitbrecht, V., and Boes, R. M. (2016). "Measuring bed load transport rates by grain-size fraction using the Swiss plate geophone signal at the Erlenbach." *J. Hydraul. Eng.*, 10.1061/(ASCE)HY.1943-7900.0001090, 04016003.
Zimmermann, A. E., Church, M., and Hassan, M. A. (2008). "Video-based gravel transport measurements with a flume mounted light table." *Earth Surface Processes Landforms*, 33(14), 2285–2296.